E14-2002-243

A. Yu. Didyk*, S. N. Dmitriev, Yu. N. Cheblukov[1],
A. Hofman[2], V. K. Semina, A. L. Suvorov[1], V. A. Altynov

EVOLUTION OF THE SURFACE STRUCTURES OF SOLIDS UNDER IRRADIATION WITH HIGH ENERGY HEAVY IONS

[1]Institute of Theoretical and Experimental Physics, 117259 Moscow, B. Cheremushkinskaja, 25, Russia
[2]Permanent address: Institute of Atomic Energy, Otwock-Swerck, Warsaw, Poland
*E-mail address: didyk@main1.jinr.dubna.ru

1. INTRODUCTION

Research on the influence of irradiation with swift heavy ions has been carried out intensively for the last 10-15 years practically at most accelerator centers. As is well known, the problems of ion track creation were connected with two old models: a Coulomb explosion model and a thermal spike (thermal peak) one. With the development of some new methods for the study of irradiated surfaces, such as scanning tunneling (STM) and atomic force microscopy (AFM), the possibilities of irradiated surface investigations gained a new life.

It is very interesting to study the interaction of swift heavy ions with metals, dielectrics, semiconductors and with amorphous metals. The structure of amorphous metals is very interesting, indeed. It is characterized by only a short-range order in atomic arrangement without a long-range order. So the free electrons have a small projected range around the ion trajectory and as a result can release enough energy for the yielding temperature higher than necessary for thermal peak and higher than melting point or evaporation temperature for a given material.

The purpose of this article is to verify these models and to study the role of each model in the surface structure evolution. We carried out the research on surface structure changes during ion irradiation of some metals, high-oriented pyrolytic graphite (HOPG) and amorphous metal alloys.

2. SPUTTERING OF METALS WITH SWIFT HEAVY IONS AT HIGH FLUENCES

Research on the sputtering of coarse-grained metals by heavy ions in the inelastic energy loss range was started only about ten years ago in connection with acceleration and storage requirements for high-intensity heavy ion drivers [1]. The sputtering yields of coarse-grained gold with high-energy ^{238}U and ^{84}Kr ions have been measured experimentally [2, 3], and experimental data on the sputtering of Au, Zr and Ti by Au swift ions has been recently obtained [4]. As analysis of experimental results has shown [2-4], the difference between the experimental sputtering yield and the yield calculated according to cascade theory is generally insignificant.

In a heavy ion driver, heavy ions, which left the mode of acceleration or accumulation, will irradiate structural metal elements, where they create defects in the initial crystalline structure due to elastic collisions. These defects persist during irradiation. In this case the sputtering mechanism can be changed [5, 6]. The samples of all studied materials (Ni, W, stainless steel, amorphous alloys and pyrographite) were irradiated with the use of the set-up described recently [7, 8].

The samples of Ni, W and stainless steel (SS) were irradiated with ^{86}Kr ions [9–12]. Before irradiation all samples were annealed at 700°C for 1 h and then were electrochemically polished. Before and after irradiation the samples were characterized by means of a scanning electron microscope JSM-840.

The scanning electron microscopy (SEM) images for Ni are presented in Fig.1, where (*a*) is the unirradiated surface and (*b*) shows the surface after irradiation with 305 MeV ^{86}Kr ions up to fluence $F \cdot t = 2 \times 10^{15}$ ion/cm^2. One can see that the metal surfaces were polished by irradiation, and surface irregularities are sputtered. Furthermore, from Fig.1 it is possible to see a considerable material sputtering near the grain boundaries. The yield of the grain boundary sputtering S is more than 2000 atom/ion. The sputtering yield has been estimated by approximating the volume of the material sputtered on grain boundary.

To estimate sputtering yield for grain body, a nickel sample was irradiated up to the fluence $F \cdot t = 2 \times 10^{15}$ ion/cm^2 using a mask. The mask was placed over the half of the irradiated surface and then the exposed area was reirradiated with 245 MeV ^{86}Kr ions up to the fluence of $F \cdot t = 1 \times 10^{15}$ ion/cm^2. The thickness of the sputtered material layer, which is equal to difference between thickness for the single- and double-irradiation parts of the nickel sample (see Fig.2), was $h \approx 0.35$ μm, which allowed one to estimate a sputtering yield as $S_{Ni} = 3000$ atom/ion.

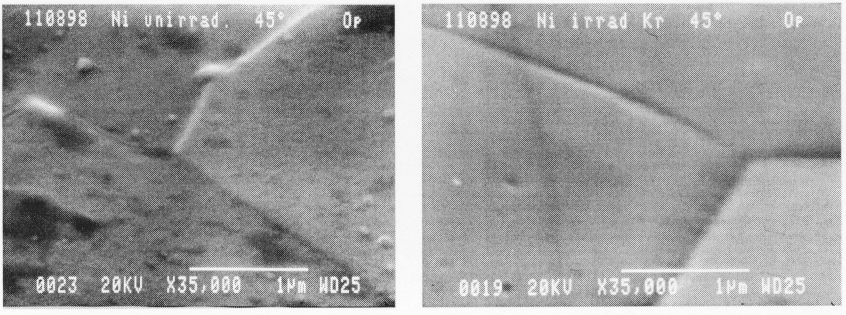

a *b*

Fig.1. The surface structure of polycrystalline Ni before (*a*) and after irradiation (*b*) with 305 MeV ^{86}Kr ions up to fluence $F \cdot t = 2 \times 10^{15}$ ion/cm^2. The images were obtained using SEM technique

Double irradiation allowed one to decrease possible swelling influence on the estimation of the experimental sputtering yield. In this experiment, the swelling of Ni can only decrease estimations of the sputtering yield. More high yield of grain boundary sputtering can be explained by its initially defected crystal structure.

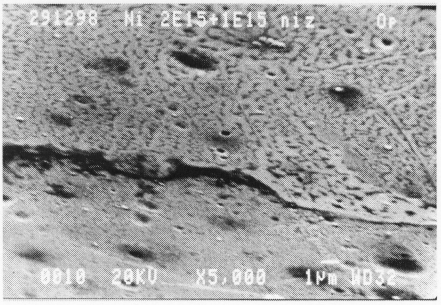

Fig.2. The surface structure of polycrystalline Ni previously irradiated with 305 MeV ^{86}Kr ions up to fluence $F \cdot t = 2 \times 10^{15}$ ion/cm^2 and then irradiated with 245 MeV ^{86}Kr ions up to the fluence of $F \cdot t = 1 \times 10^{15}$ ion/cm^2 (the upper part was covered by mask). One can see a step on the boundary between single- and double-irradiated regions

The presence of radiation defects in metals essentially increases the influence of inelastic energy loss of swift heavy ions on the sputtering yield. Thus, the sputtering yield for the metal having a low defect concentration in the crystalline structure is in the range of 1-10 atom/ion [3-5]. Experiment [9] has shown that the sputtering yield for coarse-grained metals with swift heavy ions increases by a factor of 10^2-10^3 at high irradiation fluences ($F \cdot t = 2 \times 10^{15}$ ion/cm^2) at the expense of accumulating radiation defects in the target crystalline structure. The high sputtering yield for nickel observed experimentally is possibly explained by atom evaporation from the ion track surface, which has been heated up to temperature higher than a boiling point. The observed effects can be understood on the basis of the model that will be presented below.

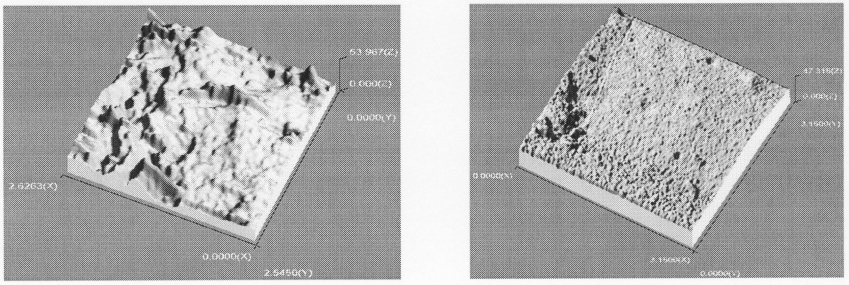

a *b*

Fig.3. The nickel surface structures in initial sample (*a,* the scanning area is 2.6 μm × 2.6 μm and height is 54 nm) and after irradiation with 305 MeV Kr ions up to fluence $F \cdot t = 2 \times 10^{15}$ ion/cm^2 (*b*, the scanning area is 3.15 μm × 3.15 μm and height is 47 nm). The images were obtained by means of STM technique

The STM-images of the surface structure for Ni grain body are presented in Fig.3. One can see the initially electrochemically polished nickel surface

structure before irradiation (*a*) and after irradiation (*b*) with 305 MeV ^{86}Kr ions up to fluence $F \cdot t = 2 \times 10^{15}$ ion/cm^2. The images (scans) were obtained by the STM technique.

The difference between the heights of relief for unirradiated (*a*) and irradiated (*b*) samples, as one can see from Fig.3, is very high: 53.97 nm and 11.66 nm, respectively. We calculated the mean height values using a lot of scans for unirradiated (*a*) and irradiated (*b*) nickel. These values turned out to be H_a=46.97 nm and H_b=21.15 nm. The approximating number of atoms, N_{NiS}, evaporated (sputtered) from the nickel surface under the irradiation with ^{84}Kr ions has been estimated by means of simple expression

$$N_{NiS} \sim (H_a - H_b) \cdot N_{Ni} = 2.36 \times 10^{17} \text{ atom/cm}^2, \qquad (1)$$

where $N_{Ni} = 9.125 \times 10^{22}$ atom/cm^3 is the number of atoms per 1 cm^3. So the sputtering coefficient (or, most probably, evaporation coefficient) has an approximating value $S_{ex} \cong N_{Ni}/F \cdot t = 1.2 \times 10^2$ atom/ion.

As is very easy to estimate, the pressure in the area around the hot ion track in metals at the temperatures about $T_{tr} \sim 10^4$ K (without any volume changes) must be approximately 10^2 kbar [51, 52]. So the target atoms can be thrown out from the surface by high pressure, too. Time for energy transfer from electrons heated with heavy ions to lattice atoms is $t \approx 10^{-12}$ s, and lattice atoms cannot obtain high temperature [14]. In the case of crystal with the high defect concentration, the energy transfer time can decrease down to 10^{-13} s and the temperature of the lattice around the ion trajectory must be very high. It can cause lattice melting and ion track creating. The final temperature on the track axis may be estimated with the help of expression [14]

$$T(0) = \{4 \cdot h \cdot S^2 \cdot N \cdot \sigma_0 \cdot \alpha \cdot r_0^2 \cdot T_0^{1/2} \{(T_0/\varepsilon_F)^{1.5} - 1\}/(9 \cdot a \cdot \beta)\}^{1/2}. \qquad (2)$$

Here $\sigma_0 = 2 \cdot \pi \cdot a_0^2$, a_0 is the Bohr radius, S - the acoustic velocity, N - the atom density for target material, r_0 - the initial radius of excited electrons, T_0 - the initial electron temperature in the excited area, a - the lattice constant, α and β are constants (for the Z>20 they are equal to 0.05-0.1 eV), ε_F - the Fermi energy. Using this expression, it is possible to estimate the temperature in the ion track area. The temperature estimated with the use of eq.(2) ($T_{tr} \approx 3700$ K) is higher than the nickel melting point (T_{melt}=1873 K). Thus, the processes of Ni atom evaporation must take place with the increasing of damage concentration. And this fact allows one to understand such a high sputtering yield for Ni.

Study of the sputtering yield for W single crystal and stainless steel Cr18Ni10 (SS) was carried out for comparison. And the chemical element composition of irradiated SS was determined too.

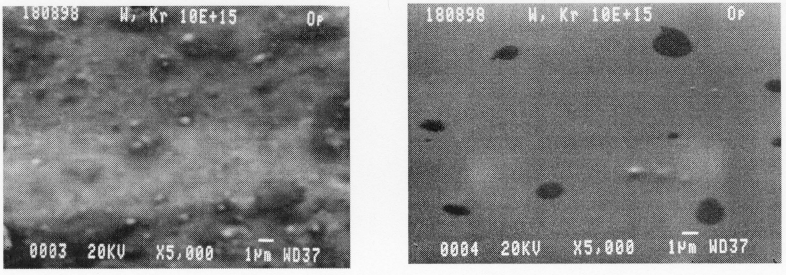

a *b*

Fig.4. The surface structures of single tungsten crystal before (*a*) and after (*b*) irradiation with 305 MeV ^{86}Kr ions up to the fluence $F \cdot t = 2 \times 10^{15}$ ion/cm^2. The images were obtained using SEM technique

The surface structures of tungsten single crystal before (*a*) and after (*b*) irradiation with 305 MeV ^{86}Kr ion up to fluence $F \cdot t = 2 \times 10^{15}$ ion/cm^2 are presented in Fig.4. The images were obtained by scanning electron microscopy (SEM). The initial W single crystal exhibits a very good characteristic – the ratio of its resistivity at room temperature and that at liquid helium temperature was $\rho(300\ \text{K})/\rho(4.2\ \text{K}) = 80000$. On Fig.4 one can see the initially polished tungsten surface after Kr heavy ion irradiation.

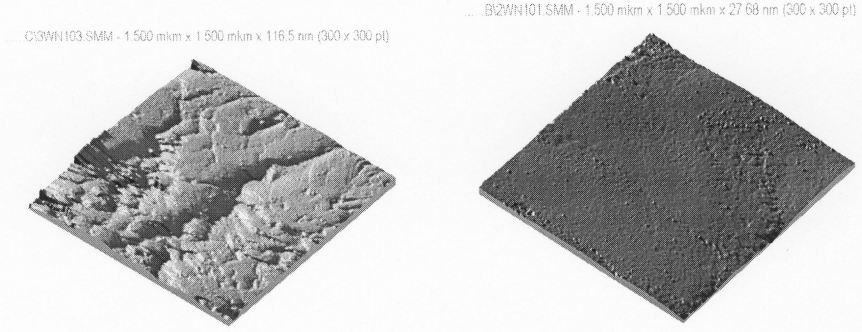

a *b*

Fig.5. The tungsten surface structures in initial state (*a*) and after irradiation (*b*) with 305 MeV Kr ions up to the fluence $(F \cdot t)_2 = 2 \times 10^{15}$ ion/cm^2. The scanning area is 1500 μm × 1500 μm. The relief heights are 116.5 nm (*a*) and 27.68 nm (*b*). The images were obtained by using of the STM technique

To estimate the surface relief inhomogeneities on small area, the scanning tunneling microscopy (STM) was used. In Fig.5 the surface structures of the initial (*a*) tungsten crystal and the one irradiated with 305 MeV Kr ions up to the fluence $F \cdot t = 2 \times 10^{15}$ ion/cm^2 (*b*) are presented. As one can see from Fig.5, the

difference between the relief height for unirradiated and irradiated sample is significant: 75.5 nm and 8.73 nm, respectively. We calculated the mean height values using a lot of scans for unirradiated (*a*) and irradiated (*b*) tungsten. These values turned out to be H_a=61.08 nm and H_b=21.96 nm. The approximating number of atoms N_{WS} evaporated (sputtered) from the metal W surface under the irradiation with ^{84}Kr ions has been estimated by means of expression (1). So one can obtain $N_{WS}\sim(H_a-H_b)\cdot N_W=2.47\times10^{17}$ atom/cm^2, where $N_W=6.32\times10^{22}$ atom/cm^3 is atom number per 1 cm^3. In such a manner the sputtering coefficient (or, most probably, the evaporation coefficient) has an approximating value $S_{ex}\cong N_{WS}/(F\cdot t)=1.23\times10^2$ atom/ion.

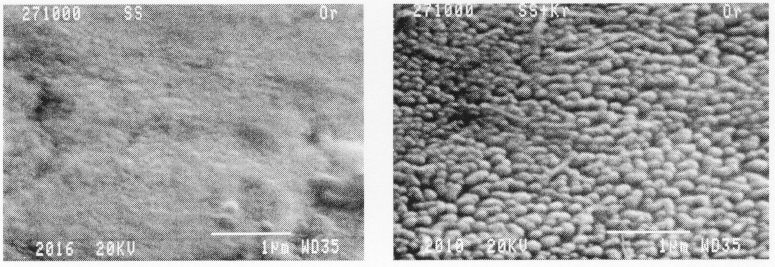

a *b*

Fig.6. The stainless steel surface structure in the initial state (*a*) and after irradiation (*b*) with 245 MeV ^{86}Kr ions up to fluence $F\cdot t=2\times10^{15}$ ion/cm^2. The images were obtained by using the STM technique

The surface structure of chromium-nickel stainless steel (Cr18Ni10) irradiated with ^{86}Kr ions is presented in Fig.6. Figures 6*a* and 6*b* show the SS surface structures in initial state and after irradiation with fluence up to $F\cdot t=2\times10^{15}$ ion/cm^2, respectively. As one can see, the irradiated surface exhibits an interesting structure. The whole irradiated area is covered by the so-called hillocks. The ion irradiation fluence was the same as in the case of Ni. Analogous surface structure of the SS irradiated with 124 MeV ^{129}Xe ions was recently observed by the authors at very high fluences [13]. The electron microprobe analysis for the SS samples irradiated with 245 MeV ^{86}Kr ion up to fluence $F\cdot t=5\times10^{15}$ ion/cm^2 was carried out with the electron scanning microscope JSM-840. It was found that the chemical compositions of SS sample change from $Fe_{69.7}Cr_{17.6}Ni_{12.7}$ to $Fe_{73.7}Cr_{19.7}Ni_{6.6}$. So the Ni content becomes about twice as much, but concentration of other elements decreases. It means that the processes of sputtering took place under irradiation.

Calculated values of projected ranges R_p and inelastic energy loss $S_{inel}=(dE/dx)_{inel}$ for the Ni, W and SS targets are presented in Table 1. These calculations were made by means of a computer code TRIM-2000. To estimate

temperature on the track axis using the calculated values S_{inel}, we used the expression which is more simple than (2) (see [13, 15]):

$$T_{tr} = S_{inel}(x)/(\pi \cdot R_{tr}^2 \cdot C_i \cdot \rho_i) + T_0. \quad (3)$$

Here C_i is a specific capacity, ρ_i - material density, R_{tr} - track radius, T_0 - irradiation temperature. We will use a simple model for evaporation: the target atoms can evaporate from the cone with the diameter D_{evap} and the depth H_{evap}, and $H_{evap} \approx D_{evap}$. Then the volume of the evaporated materials can be calculated by means of the expression

$$V = \pi \cdot D_{evap}^2 \cdot H_{evap}/12 = S_{ex}/N_{mat}. \quad (4)$$

Here S_{ex} and N_{mat} are sputtering yield and the number of atoms in 1 cm^3, respectively. The total volume of the evaporated materials was estimated from SEM- and STM-images. The explanation of such large values of sputtering yield can be carried out on the base of thermal spike model, i.e. that for all studied metals the temperatures in the area around the tracks are higher than the melting point and evaporation temperature too. As was shown in ref. [14], the temperature on the track axis at metallic single crystals cannot be higher than the melting temperature because the electron-electron interaction must dissipate the ion energy transfer to electrons on the crystal. But for crystals with high defect concentration the situation can be another. For amorphous metallic alloys this temperature may be higher than the melting and evaporation temperatures if the inelastic energy is more than threshold energy for hot ion track creation. This effect takes place at metals irradiated by high ion fluences. Thus, the evaporation processes will take place.

Table 1. TRIM-calculated values of projected range R_p, inelastic energy losses $S_{inel}=(dE/dx)_{inel}$, track temperature T_{tr}, sputtering yield K, crater diameter D_{evap} and published data about melting point T_{melt} for nickel, stainless steel (SS) and monocrystalline tungsten

Material	Ni	SS	W
R_p, μm	14.2	15.4	11.9
S_{inel}, MeV/μm	28	24.5	35
T_{tr}, K	1.04×10^4	0.95×10^4	2×10^4
T_{melt}, K	1728	1673	3693
K, atom/ion	>120	>100	>120
Crater diameter, D_{evap}, Å	>17	>16	>20

In ref. [15] the estimations for tracks in Fe irradiated with fission fragments (energy of fragments such as krypton and xenon is about 1 MeV/amu) were carried out and the estimated track temperature was about $T_{tr} \approx 6000$ K.

Thus, one can conclude that the thermal spike model at damaged materials can explain the high value of sputtering yield for some metals irradiated with swift heavy ions up to high fluences.

3. STRUCTURAL CHANGES IN AMORPHOUS ALLOYS UNDER IRRADIATION WITH SWIFT HEAVY IONS

The study on structural changes and other properties of amorphous metal alloys irradiated with swift heavy ions is really of great interest for a number of reasons. First of all, such systems do not have a long-range order in atomic arrangement and exhibit only a short-range order. Practically amorphous systems are disordered materials.

The investigations of amorphous alloys under heavy ion irradiation attract interest of specialists [16-23]. The main results were the following:

1. Under irradiation with heavy ions, the dimensions of samples perpendicular to the ion beam direction increased, but the sample dimension along the ion beam shrunk.
2. The processes of sputtering did not take place practically.
3. These irradiation-induced dimension changes were not accompanied by volume changes.
4. The consistent studies of sputtering yields of metallic amorphous alloys were not carried out.

The purpose of this paragraph is to study the radiation phenomena in amorphous alloys such as $Ni_{58}Nb_{42}$, $Fe_{67}Ni_2Si_{14}B_7$, $Fe_{83}Si_{13.5}B_{3.5}$ and $Ta_{37}Ni_{63}$ at high fluences of heavy ions [24, 25].

The samples of amorphous alloys $Ni_{58}Nb_{42}$, $Fe_{83}Si_{13.5}B_{3.5}$ and $Ta_{37}Ni_{63}$ were irradiated with 245 MeV ^{84}Kr ions up to the fluences 10^{14} and 10^{15} ion/cm^2 and 710 MeV ^{209}Bi ions up to the fluences 10^{12} and 10^{13} ion/cm^2. The irradiation temperature was less than 100°C. The irradiation was carried out at the installation which was described in [7, 8]. The mean ion beam intensities (flux) were $F<10^{11}$ ion/(cm^2·sec) or less.

The initial surface of $Ni_{58}Nb_{42}$ sample is presented in Fig.7*a*. One can see the structural defects on the surface - the frozen melt drops.

The surface structure of irradiated amorphous alloy $Ni_{58}Nb_{42}$ is presented in Fig.7(*b*, *c*). One can see that at temperature $T \cong 300$ K the samples changed strongly. The areas with the freezing melt drops practically kept the position on the surface, but the relatively smooth area around these drops was displaced along ion bombardment direction so that the drops became immersed under the

smooth surface part. The swelling value of samples irradiated with 245 MeV ^{86}Kr ions at $F \cdot t = 10^{15}$ ion/cm^2 is found to be $\Delta V/V \sim 15\%$. And the chemical composition on the sample surface is found to change, too. The alloy chemical composition can be expressed as $Ni_{58-x}Nb_{42+x}$, where $x=1.60$ at ion fluence $F \cdot t = 10^{15}$ ion/cm^2 and $x=1.48$ at ion fluence $F \cdot t = 10^{14}$ ion/cm^2. One can conclude that the significant changes of chemical composition at relatively low fluences must be caused by evaporation processes of rather Ni than Nb atom as the latter is more refractory atom.

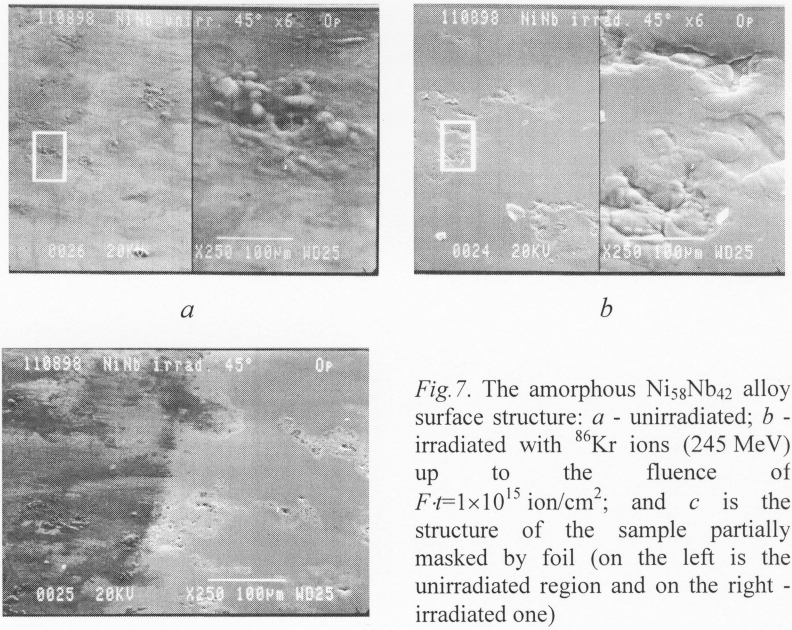

a *b*

c

Fig.7. The amorphous $Ni_{58}Nb_{42}$ alloy surface structure: *a* - unirradiated; *b* - irradiated with ^{86}Kr ions (245 MeV) up to the fluence of $F \cdot t = 1 \times 10^{15}$ ion/cm^2; and *c* is the structure of the sample partially masked by foil (on the left is the unirradiated region and on the right - irradiated one)

In Fig.8 the $Ni_{58}Nb_{42}$ surface structures obtained by scanning tunneling microscopy are presented. One can see that the volume increasing is connected with the multistep volume growth, but not with surface growth. The projected range of ^{86}Kr ions in $Ni_{58}Nb_{42}$ alloy is $R_p = 13.4$ μm (the density of this alloy is $\rho = 8.54$ g/cm^3, the threshold energy for damage creation $E_d \cong 30$ eV). The inelastic energy loss is $(dE/dx)_{inel} = 24$ MeV/μm and the damage doses created in the processes of the elastic collisions are $D_{el} = 0.037$ dpa and $D_{el} = 0.0037$ dpa for the ion fluences 10^{15} and 10^{14} ion/cm^2, respectively; the cross section of target atom displacement is $\sigma_{el} = 3.7 \times 10^{-17}$ dpa·cm^2/ion.

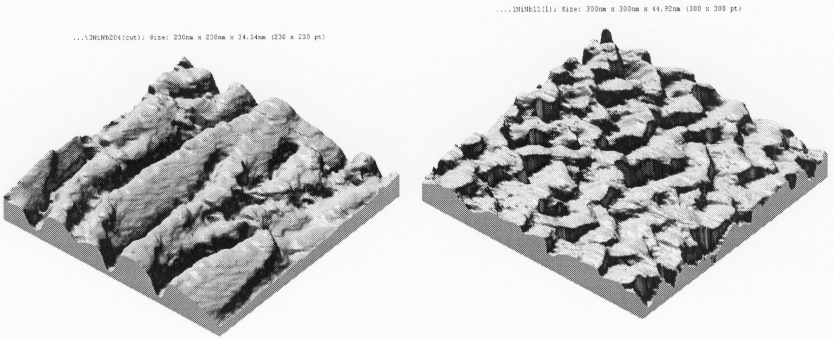

a *b*

Fig.8. The structure of amorphous $Ni_{58}Nb_{42}$ alloy irradiated with 245 MeV ^{86}Kr ions up to the fluence $F \cdot t = 1 \times 10^{15}$ ion/cm^2 (*b* – 300 nm ×300 nm × 44.9 nm) and unirradiated (*a* – 230 nm × 230 nm × 34.5 nm). The structures were obtained with the STM technique

The temperature around ion track can be calculated using some publications [9, 26-28]. The temperature peak (thermal spike) model was used for description of the radiation phenomena under irradiation with swift heavy ions of solids (e.g. [26]). This model is based on earlier publications [27, 28]. The expressions have the form

$$C_e \cdot (dT_e/dt) = \nabla K_e \nabla T_e - \alpha \cdot (T_e - T_i) + A(\rho, t), \quad (5a)$$

$$C_i \, (dT_i/dt) = \nabla K_i \nabla T_e + \alpha \cdot (T_e - T_i). \quad (5b)$$

Here C_e and C_i are specific capacities for electrons and lattice atoms, and K_e and K_i are electronic conductivity and lattice conductivity, respectively; C and K are temperature-dependent parameters; α - the constant of electron-phonon interaction. The electronic temperature can be estimated by means of expressions [27]

$$T_e(\rho) = 4(dE/dx)_{inel}/(\pi \cdot C_e \cdot \rho^2) \cdot \exp(-\rho/\rho_e^2). \quad (6)$$

If parameters C_e, C_i, K_e and K_i do not depend on temperature, the solution of system (5) can be written in the form [27]

$$T_i(\rho,t) = \alpha \, (dE/dx)_{inel}/(2 \cdot \pi \cdot C_e \cdot C_i) \cdot \int \{\exp(-\omega_1 t) - \exp(-\omega_2 t)\} \times$$
$$\times \exp(-k\rho_e)^2 \cdot J_0(k\rho) k dk/(\omega_2 - \omega_1), \quad (7)$$

parameters ω_2 and ω_1 are presented in ref. [27].

The using of expressions (2), (3), (5) and (7) allows one to estimate the temperature on the axis of Kr ion track in amorphous alloys. The temperature is

T_{tr}≅4000 K and it is higher than the melting point and the evaporation temperature for this material. So in this system the evaporation (sputtering) processes must take place.

4. THE CHANGES OF SURFACE STRUCTURE OF HIGHLY ORIENTED PYROLYTIC GRAPHITE (HOPG) IRRADIATED WITH SWIFT HEAVY IONS

The results of this review paragraph are the continuation of the cycle of publications on the influence of high inelastic energy losses of swift heavy ions on the structure and properties for conductive polycrystalline materials (e.g. [1-6]) and for HOPG [29-34]. First of all, such studies are also important for understanding the fundamental laws of charge particles interaction with solids; secondly, they have gained applications for the construction and creation of nuclear physics accelerators, reactors and heavy ion drivers to solve problems related to creating thermonuclear fusion reactors [2].

In ref. [35] on the surface of HOPG irradiated with 10-100 MeV ^{40}Ar ions a lot of hillocks were observed. A characteristic hillock diameter was less than 3 nm. The hollows (craters) were found on the hillock peaks. In the work [35] the hillock creation was connected with the inelastic energy losses $(dE/dx)_{inel}$=5 keV/nm for Ar ions, but no explanation of hollows creation has been provided yet.

This part gives the results of our studies about HOPG surfaces irradiated with 305 MeV ^{86}Kr and 705 MeV ^{209}Bi ions by air STM [36, 37]. The possibilities of high resolution STM allow us to study ion effect on a surface structure at low ion fluences (about 10^{11}-10^{12} ion/cm^2).

The STM image of HOPG surface before (*a*) and after irradiation (*b*) with 305 MeV ^{86}Kr ions at the fluence of 5×10^{12} ion/cm^2 is presented in Fig.9. Part of the sample surface was covered by a special mask and did not irradiate, while the other one was irradiated with ions. Then the grain boundaries were studied in detail with the use of STM technique. On the unirradiated part of the HOPG sample one can see a boundary between two crystal grains, while on the irradiated part one can see a strongly sputtering boundary. The boundary depth in Fig.9(*a*) is estimated to be 5 Å, while in Fig.9(*b*) it is equal to 47 Å. So, it is easy to see here, that the boundary sputtering predominates over body grain sputtering. For grain boundaries the sputtering coefficient is very high. It means that the ^{86}Kr ions produce the hot tracks connected with the high inelastic energy loss $(dE/dx)_{inel}$≅10 MeV/μm in the area where the crystal structure has high defect concentration and is disordered. The hot tracks on and near the surface have temperature higher than the sublimation and evaporation temperatures for graphite.

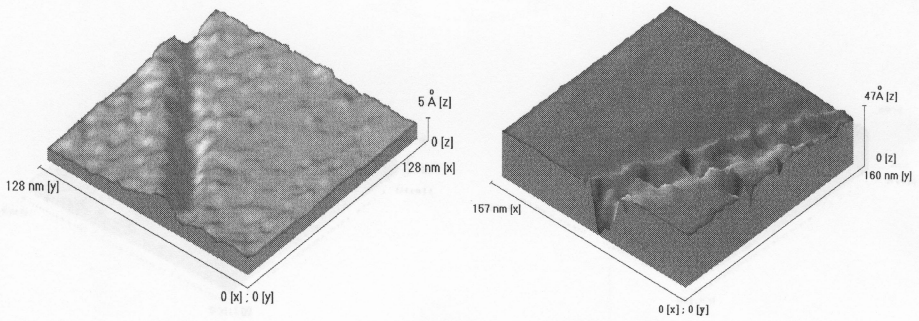

a *b*

Fig.9. The STM-images of initial (*a*) and irradiated with 305 MeV ^{86}Kr ions up to fluence 5×10^{12} ion/cm^2 (*b*) HOPG surfaces. The scanning areas are 128 nm × 128 nm (*a*) and 167 nm × 160 nm (*b*) and the vertical sizes are 5 Å (*a*) and 47 Å (*b*)

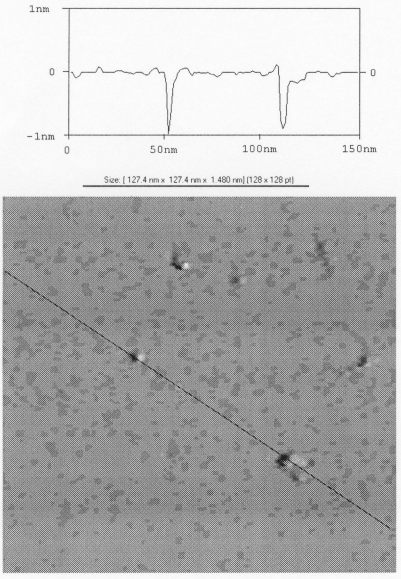

Fig.10. The STM-image of the HOPG surface structure irradiated with 705 MeV ^{209}Bi ions up to the fluence of 10^{12} ion/cm^2. On the top figure one can see the scanning profile along the line shown on the bottom figure

The STM image of HOPG irradiated with ^{209}Bi ions at the fluence 10^{12} ion/cm^2 with energy 705 MeV is presented in Fig.10. One can see the craters which were formed on the surface of individual HOPG grain after ^{209}Bi ion irradiation. The analysis of all STM images has shown that the mean surface crater concentration is only about 2-3% of the total ion fluence (10^{12} ion/cm^2). This means that the crater creation process is probable, i.e., is related to thermal fluctuations and only a small part of ions can produce the hot tracks in which the temperature is high enough to evaporate carbon atom. The

predominant character of boundary sputtering under irradiation with Kr ions allows us to explain this fact. The craters can be created in the volume near the surface of material in which HOPG grains have local surface disordered crystalline structure. The small craters on some hillocks with diameter ≈3 nm under irradiation with 10-100 MeV Ar ions [35] can be explained by the same phenomenon. Inelastic energy losses for 705 MeV ^{209}Bi ions and for 10-100 MeV ^{40}Ar ions are equal to $(dE/dx)_{inel}$ ≅27 MeV/μm and $(dE/dx)_{inel}$ ≅5 MeV/μm, respectively. It is a reason for a bigger crater diameter in case of ^{209}Bi ions in comparison with crater production under ^{40}Ar ion irradiation.

It is well known that hillocks under HOPG irradiation with 3 MeV/amu heavy ions are of fluctuation character and very small sizes: their height is <0.5 nm and the diameter is ≈1 nm [38, 39]. At our experiments the scanning step was 10 Å, and as a result it was impossible to observe the hillocks on the HOPG surface (see Fig.9).

A cylindrical region of excited electrons will be formed around the ion trajectory in a solid target. The radius of this region is r_0~10 Å and initial electron gas temperature is about 20-40 eV [14]. The relaxation of excited electrons will be owing to electron-electron collisions (electron thermal conductivity) and electron-lattice interactions, which can lead to lattice atom heating. In the HOPG case the excited electron region cooling based on electron thermal conductivity will be strongly straitened because the free electron density for single crystal graphite is practically by three orders of magnitude less than that in metals and has a value ≈5×10^{18} electron/cm^3 [40]. Thus, a significant part of excited electron energy will be transferred to ionized lattice atoms and this phenomenon takes place in a cylindrical excited electron region. However it does not lead to hot track formation because the HOPG has high lattice thermal conductivity. Fig.11 shows the dependence of HOPG lattice thermal conductivity χ_L in direction parallel to surface versus the lattice temperature. The dependence of lattice thermal conductivity χ_L was calculated on the basis of published data [40]. The characteristic time for energy transfer from electrons excited by ion to lattice atoms is equal to $\tau_h \approx 10^{-12}$ s [41].

The characteristic time for HOPG atoms cooling in a wide temperature T_L range (up to 1000 K) as a result of lattice thermal conductivity must be $\tau_L \approx r_0^2/\chi_L < 10^{-14}$ sec. The condition $\tau_L << \tau_h$ means that the lattice atoms will not be heated and fast heavy ions will not create hot tracks and, respectively, the craters will be absent on the surface. On the boundaries between the crystal grains and in the positions with a local disordered crystalline structure the condition $\tau_L << \tau_h$ will be disturbed. Firstly, τ_h decreases down to ~10^{-13} s [14, 41]. Secondly, the lattice thermal conductivity and, respectively, the temperature conductivity strongly decrease, too. As a limit case for the amorphous graphite its heat conductivity is two orders of magnitude less than

that for HOPG [42]. So in the process of fast heavy ion passing through the regions with strongly defected crystalline structure the hot track formation and carbon atom evaporation from the surface will be observed.

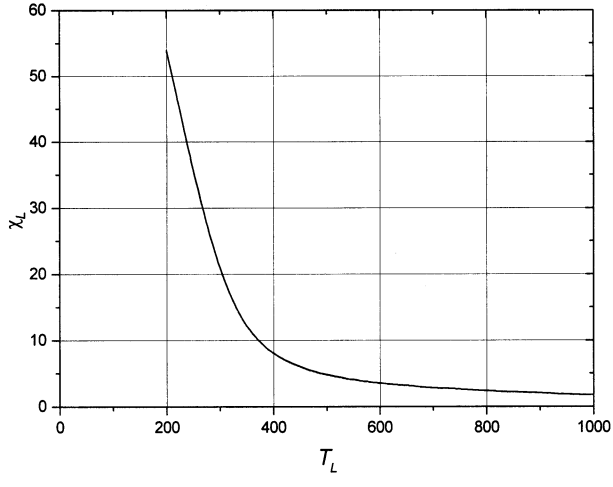

Fig.11. The HOPG lattice thermal conductivity χ_L in direction parallel to the surface as a function of the lattice temperature

5. THE SPUTTERING OF GOLD IRRADIATED WITH SWIFT HEAVY IONS

The sputtering coefficients for annealed gold foils irradiated with ^{238}U, ^{196}Au and ^{86}Kr swift heavy ions are presented in Table 2 [3–6]. As one can see, the experimental values of the sputtering coefficient are S_{ex}≈1-12 atom/ion. The Au sputtering coefficients calculated with the help of the cascade sputtering model, $S_{C.T.}$, differ substantially from experimental values, especially for irradiation with ^{238}U and ^{196}Au ions with high level of inelastic energy losses. The projected ranges of ^{238}U, ^{196}Au and ^{86}Kr ions in Au, the elastic cross-section near the surface σ_d and inelastic energy losses $(dE/dx)_{inel}$ are presented in Table 3.

At the calculations of Au atom displacement under elastic collisions σ_d with ions, the threshold energy was taken as E_d=20 eV (see Table 3).

As one can see, the elastic cross-section of the Au atom displacement has the biggest value in the case of irradiation of annealed gold thick foil with ^{196}Au ion, but the sputtering coefficient S_{ex} is less in comparison with irradiation with ^{238}U ions: 9.3 atom/ion and 12 atom/ion, respectively. This difference between

the sputtering coefficients can not be explained by using only elastic collisions. It is necessary to take into account also the inelastic energy losses and the temperature effects (thermal spike model). The inelastic energy losses $(dE/dx)_{inel}$ for ^{238}U are more than those for ^{196}Au ion irradiation by a factor of ~1.8.

Table 2. The experimental sputtering yield in the inelastic energy loss range for the gold polycrystalline targets irradiated with heavy ions

Ion/Material	Energy, MeV	Sputtering yield experiment, S_{ex}, atom/ion	Sputtering yield, cascade theory, $S_{C.T.}$, atom/ion	Inelastic energy losses, $(dE/dx)_{inel}$, keV/Å
$^{238}U/^{196}Au$	1400	12±2	≤1	9.82
$^{196}Au/^{196}Au$	230	9.3±0.9	~3	5.52
$^{84}Kr/^{196}Au$	200	1.0±0.2	≤1	3.28

Table 3. The calculation values of projected ranges, R_p, elastic cross-section near the surface, σ_d, and inelastic energy losses, $(dE/dx)_{inel}$, for some ions in Au

Ion/Material	Energy, MeV	Projected range, R_p, μm	Inelastic energy losses, $(dE/dx)_{inel}$, keV/Å	Elastic cross-section, σ_d, dpa·cm^2/ion
$^{238}U/^{196}Au$	1400	21.26	9.82	$3.7\cdot10^{-16}$
$^{196}Au/^{196}Au$	230	7.65	5.5	$1.1\cdot10^{-15}$
$^{84}Kr/^{196}Au$	253	10.78	3.33	$1.65\cdot10^{-16}$

Then the gold samples underwent cold deformation to create high concentration of dislocations as drawing defects (the gold purity was 99.0%) were irradiated with 253 MeV ^{84}Kr ions up to 10^{14} ion/cm^2. The mean ion flux was 3.7×10^9 ion/(cm^2·s) during irradiation. The images of initial (*a*) and irradiated with ^{84}Kr ions (*b*) surface structures of gold samples obtained with the help of STM are presented in Fig.12. As one can see, the mean relief height in images (*a, c*) and (*b, d*) is $H_a \cong 27.19$ nm and $H_b \cong 11.66$ nm, respectively. The approximating number of atoms evaporated (sputtered) from the gold surface under ^{84}Kr ion irradiation has been estimated by simple expression (1):

$$N_{SAu} \sim (H_a - H_b)\times N_{Au} = 9.17\times10^{16} \text{ atom/cm}^2, \quad (8)$$

where N_{Au}=5.903×10^{22} atom/cm^3 is the atom number per 1 cm^3. Thus, the sputtering coefficient (or, most probably, the evaporation coefficient) has an approximating value $S_{ex} \cong N_{Au}/(F \cdot t)$=9.17×10^2 atom/ion. Comparison between the sputtering/evaporating coefficients for annealed (the first case) and cold-deformed (the second case) gold samples irradiated with Kr ions shows that they differ by a factor of ≈900.

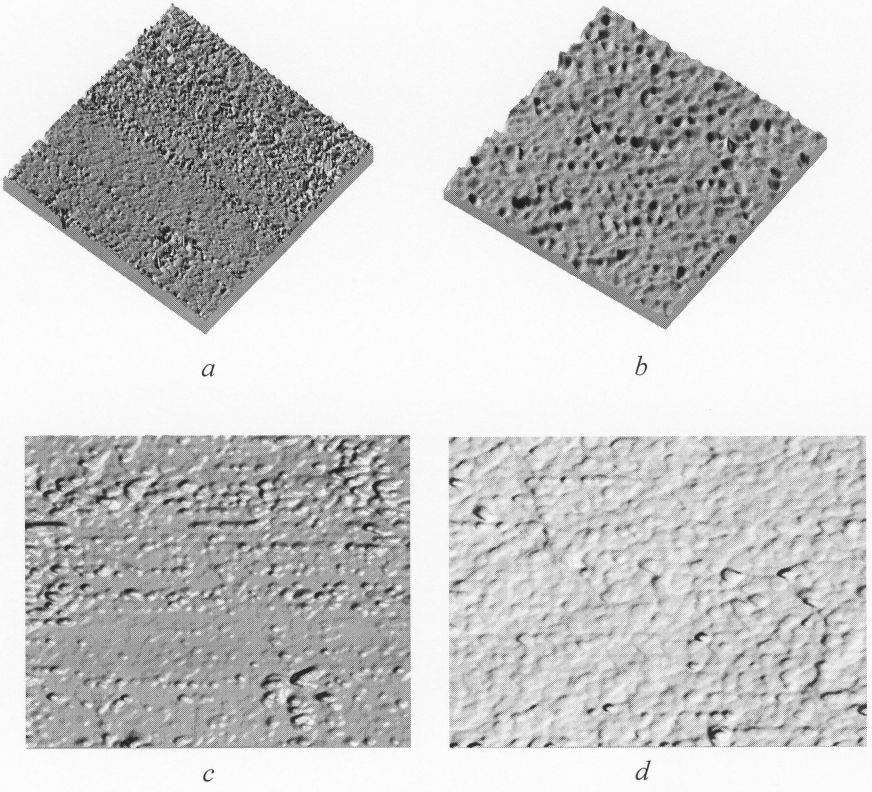

Fig.12. The STM-images of good polished initial (*a, c*) and irradiated (*b, d*) with 253 MeV ^{86}Kr ions up to fluence 10^{14} ion/cm^2 gold surfaces. The areas of scanning and the heights of relief have the values: *a*) 600 nm×600 nm×30.87 nm; *b*) 556 nm×556 nm×8.66 nm; *c*) 600 nm×600 nm×25.79 nm; *d*) 1200 nm×1200 nm×7.54 nm

Such a high value of the evaporating coefficient in the second case can be explained only by the processes of gold atom evaporation from the surface under the Kr ion passing through the surface. This means that the temperature in the volume around swift heavy ion projected range in the cold-deformed gold

samples was higher than the melting point and the evaporation temperature. So the thermal spike model must be valid in this case. The approximating temperature in the volume around the ion track may be calculated using expression (4) and the equation from [43]:

$$T_{tr}(r,t) = S_{inel}/(4\cdot\pi\cdot\chi_L\cdot t)\cdot\exp\{(-C_i\cdot r^2)/(4\cdot\chi_L\cdot t)\} + T_0, \qquad (9)$$

where T_0 is the irradiation temperature (room temperature). To calculate the temperature, we used the following parameter values: heat conductivity χ_L=270 W/(m·K) at temperature T=1000 K and heat capacity C_i=159 J/(kg·K) at temperature T=1500 K. So, we took into account the parameter value for a high temperature. Using the expression (4) and the mean value for the crater diameter on the surface of cold-deformed gold samples irradiated with ^{86}Kr ions (see Fig.11*b*) was calculated: $D_{cr}\approx$40 Å. One can obtain the temperature at the volume around the ion trajectory, ion track, from the expression (3): $T_{tr}\approx$23000 K for the track diameter D_{tr}=100 Å. The melting point and evaporation temperature for gold are much less, i.e. 1336 K and 3150 K, respectively.

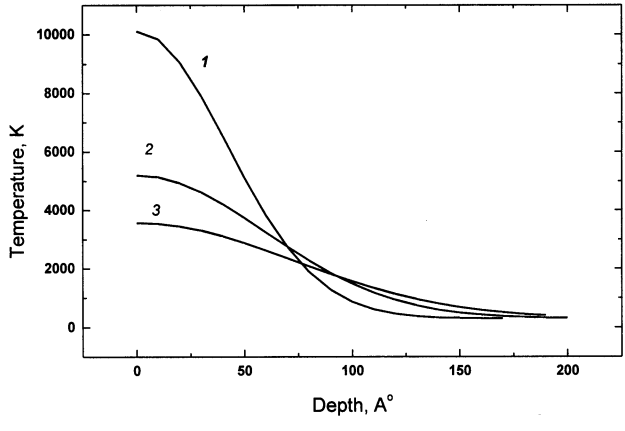

Fig.13. The temperature versus of the distance from the ion track axis for the various times: *1* - t_1=1×10^{-13} s; *2* - t_2=2×10^{-13} s and *3* - t_3=3×10^{-13} s

In Fig.13 the temperature as a function of the distance from beam trajectory axis is presented for various time t (see [43] and equation (9)). The curves *1-3* were obtained using expression (9) [10, 11]. As one can see, the temperatures at the area around the track axis with the radius about 50-75 Å

during the time up to 10^{-12} s are higher than the melting point and evaporation temperatures.

One can conclude that the sputtering/evaporation coefficient strongly depends on the defect concentration (point defects, defect clusters and drawing defects-dislocations). That conclusion is in agreement with the results obtained for irradiated metals, alloys and HOPG. The experimental results can be explained by hot electron free path decreasing. Also the condition $\tau_L << \tau_h$ (see paragraph 4) will be disturbed and τ_h decreases down to $\sim 10^{-13}$ s. The lattice thermal conductivity and consequently the temperature conductivity strongly decrease, too.

6. CONCLUSION

The presence of radiation defects in metals essentially increases the influence of inelastic energy losses of fast heavy ions on the sputtering yield. Thus, the sputtering yield for metal having a small defect number in its crystalline structure is in the range 1-10 atom/ion [3-6]. Experiments show that the sputtering yield for coarse-grained metals under swift heavy ion irradiation at high irradiation fluences ($\sim 2 \times 10^{15}$ ion/cm^2) increases significantly at the expense of accumulating radiation defects in the target crystalline structure. The experimentally observed high sputtering yield for nickel can be explained by atom evaporation from the track surface which has been heated up to boiling temperature (T_b) (i.e. a thermal spike). In this way we experimentally prove that inelastic energy losses $(dE/dx)_{inel}$ of fast heavy ion have a strong influence on sputtering the metal with a damaged crystal structure. The hot electron plasma model [44] does not contradict the experimental result given in this work.

The scanning electron microscopy studies show strong inhomogeneity of the metal surface sputtering with fast heavy ions. The sputtering yield near the grain boundaries is greater than that from the grain bodies.

Thus, the experimental research on swift heavy ion action on the surface of metals, metallic alloys, amorphous alloys and HOPG in inelastic energy loss region was carried out. The explanation of experimental results is given, too. On the base of data obtained for Ni, Au and HOPG we have concluded that track formation and consequently the high evaporation (sputtering) coefficients take place in case of high-disordered systems or in materials with relatively low concentration of free electrons (like dielectrics and some semiconductors). It has been shown that for conductive materials, when the condition $\tau_L << \tau_h$ takes place in low-defect zone, the lattice atoms around the swift heavy ion trajectory are cold and do not create a hot track. The condition $\tau_L << \tau_h$ is disturbed on the boundaries between grains and also in the area with high defect concentration, as one can see for Ni previously irradiated with high fluence (so-called "step" method, Fig.2) and for previously strongly deformed Au. As a result, when fast

heavy ion passes through such areas, a hot track is created, and the target atom evaporation takes place.

This conclusion is proved by the result of the studies about track formation in single-crystal InP semiconductor [44, 45] irradiated previously with 5 MeV electrons (fluence 5×10^{17} electron/cm^2) and then with 250 and 340 MeV ^{129}Xe and 245 and 210 MeV ^{86}Kr ions. Heavy ion tracks were also found in amorphous Si and Ge [46]. The processes of damage concentration saturation in some materials (like Ge, C, W, etc.) versus swift heavy ion fluence were observed in a cycle of publications (see, e.g., [47]). A model of disordering and following crystal recrystallization under heavy ion irradiation was developed in ref. [48, 49].

In the ref. [35] the hillocks creation on the HOPG surface was connected with the inelastic energy loss. However, this conclusion is not proved properly. The inelastic energy loss cannot have influence on the HOPG surface structure changes except for the regions with a defected crystal lattice. The hillock creation can be explained on the base of elastic energy losses of heavy ions, which can produce collision cascades with displacement of lattice atoms and the following processes like HOPG swelling in the place of ion passing through the surface.

For the preparation of heavy ion program for CERN (LHC), accumulation and cooling tests with lead ion beams have been performed in the LEAR storage ring. These tests have revealed that, due to the unusually large outgassing of the vacuum system, the dynamic pressure of the ring could not be maintained low enough to reach the required beam intensities. An experimental program has been initiated for measuring the molecular desorption yields of stainless steel vacuum chamber by the impact of 4.2 MeV/amu lead ions with the charge stage +27 and +53. The test chamber was exposed either to grazing or to perpendicular incidence. Different surface treatment was reported in terms of the molecular desorption yields for H_2, CH_4, CO, CO_2. Unexpectedly large values of molecular yields per incident ion up to 2×10^4 molecules/ion have been observed [50].

The hillock structures which look like the semi-sphere appear on the stainless steel surface irradiated with ^{86}Kr ions (the energy is 245 MeV and the fluence is 2×10^{15} ion/cm^2). These structures are similar to the structures which appear on the surface at the blistering phenomenon. It means that the surface begins to accumulate the gases under irradiation, as a result the high pressure arises and the flaking phenomenon takes place too. Similar structures and also structures with flat tops and large squares were observed in ref. [53]. The surface change of silicon single crystals irradiated with ^{129}Xe ions (energy was 124 MeV and the fluence varied from 10^{14} to 2.9×10^{16} ion/cm^2) is presented in this work. The creation of semi-spherical hillocks and structures of another shape may be connected with the gas molecule accumulation near the surface

under the irradiation (gas desorption processes). These gas molecules could be accumulated in silicon single crystal at the processes of their growth. The creation of such hillocks on the irradiated surface allows one to explain large values of the desorption yield of gas molecules in the thermal spike model and confirms the applicability of this model.

The importance of the sputtering problem for accelerator engineering and for the high-energy heavy ion implantation into up-to-date materials makes it necessary to continue the experimental and theoretical research in high-energy heavy ions.

REFERENCES

1. P.Sigmund. Theory of sputtering. I. Sputtering yield of amorphous and polycrystalline targets // *Phys. Rev.* 1969, v.184, №2, p.383-416.
2. D.G.Koshkarev. The charge-exchange instability in intense ion beams // *Particle Accelerators.* 1984, v.16, №1-2, p.1-4.
3. Yu.N.Cheblukov, D.G.Koshkarev, A.R.Peuto *et.al.* // *Particle Accelerators.* 1992, v.37-38, p.351.
4. G.I.Akapiev, A.N.Balabaev, N.A.Vasiliev, S.V.Latyshev, V.M.Nazarov, A.R.Peuto, I.V.Rudskoy, Yu.N.Cheblukov. Gold sputtering by krypton ions in inelastic energy loss range // *J. Techn. Phys.* (Rus.). 1998, v.68, №1, p.134-135.
5. H.D.Mieskes, W.Assmann, M.Brodale, M.Dobler, H.Glückler, P.Harting, P.Stanzel. Measuring sputtering yields of high energy ions on metals // *Nucl. Instr. and Meth. in Phys. Res. B.* 1998, v.146, №1-4, p.162-171.
6. Yu.N.Cheblukov. Coarse grain structure metal sputtering by swift heavy ions in the inelastic energy loss range // *Actual problems of the nuclear physics, condensed matter physics and chemistry.* Proceedings of the 1st International School of Physics (Zvenigorod, 17-26 February 1998) / Eds. Yu.G.Abov, A.L.Suvorov, V.G.Firsov. Moscow, 1999, p.181-184 (in Russian).
7. Yu.Ts.Oganessian, S.N.Dmitriev, A.Yu.Didyk, G.G.Gulbekian, V.B.Kutner. New possibilities of the FLNR accelerator complex for the production of track membranes // *Radiation Physics of Solids.* Proceedings of the Xth International Conference (Sevastopol, 3-8 July 2000). 2000, p.42-50.
8. V.A.Skuratov, A.Illes, Z.Illes, K.Bodnar A.Yu.Didyk, A.V.Arkhipov, K.Havancsák. Beam diagnostics and data acquisition system for ion beam transport line used in applied research // *JINR Communication* E13-99-161. Dubna, 1999.
9. A.Yu.Didyk, V.K.Semina, A.Khalil, N.A.Vasiliev, A.E.Stepanov, A.L.Suvorov, Yu.N.Cheblukov. High energy heavy ion irradiation effect on nickel sputtering // *Letters to J. Tech. Phys.* (Rus.). 2000, v.26, №.2, p.1-7.

10. Yu.N.Cheblykov, A.Yu.Didyk, A.Khalil, V.K.Semina, A.E.Stepanov, A.L.Suvorov, N.A.Vasiliev. Sputtering of metals by swift heavy ions with high fluence // *Ion-Surface Interactions (ISI-2001).* Proceedings of the 15th International Conference (Zvenigorod, 27-31 August 2001). 2001, v.1, p.171-174.
11. A.Yu.Didyk, V.K.Semina, A.E.Stepanov, A.L.Suvorov, Yu.N.Cheblukov, A.Khalil. The surface structure changes of Ni, W and stainless steel irradiated with high energy krypton ions // *Advanced Materials*. 2001, №1, p.58-64.
12. Yu.N.Cheblukov, A.Yu.Didyk, A.Khalil, V.K.Semina, A.E.Stepanov, A.L.Suvorov, N.A.Vasiliev. Sputtering of metals by heavy ions in the inelastic energy loss range // *Vacuum.* 2002, v.166, № 2, p.133-136.
13. A.Yu.Didyk. Heavy ion irradiation effect on chromium-nickel steel at high temperatures // *Metals* (Rus.). 1995, №3, p.128-135.
14. Yu.Yavlinskii. Track formation in amorphous metals under swift heavy ion bombardment // *Nucl. Instr. and Meth. in Phys. Res. B.* 1998, v.146, №1-4, p.142.
15. A.A.Davydov, A.I.Kalinichenko. Mechanical effects near ion tracks and thermal peaks // *Voprosy Atomnoj Nauki i Tekhniki.* Ser.: Radiation Damage Physics and Radiation Technology (Rus.). 1985, issue 3(36), p.27-30.
16. A.Gutzmann, S.Klaumünzer, P.Meier. Ion-beam-induced surface instability of glassy $Fe_{40}Ni_{40}B_{20}$ // *Phys. Rev. Lett.* 1995, v.74, №12, p.2256-2259.
17. A.Gutzmann, S.Klaumünzer. Shape instability of amorphous materials during high-energy ion bombardment // *Nucl. Instr. and Meth. in Phys. Res. B.* 1997, v.127/128, p.12-17.
18. H.Kuch, S.Klaumünzer. Magneto-optical study of flux-line pinning in semiconductors with linear defects // *Nucl. Instr. and Meth. in Phys. Res. B.* 1998, v.146, №1-4, p.565-571.
19. S.Klaumünzer. Radiation compaction of porous Vycor glass // *Nucl. Instr. and Meth. in Phys. Res. B.* 2000, v.166-167, p.459-464.
20. Ming-Dong Hou, S.Klaumünzer, G.Schumacher. Directional changes of metallic glasses during bombardment with fast heavy ions // *Phys. Rev. B.* 1990, v.41, №2, p.1144-1157.
21. A.Meftah, M.Djebara, N.Khalfaoui, M.Toulemonde. Sputtering of vitreous SiO_2 and $Y_3Fe_5O_{12}$ in the electronic stopping power region: A thermal spike description // *Nucl. Instr. and Meth. in Phys. Res. B.* 1998, v.46, №1-4, p.431-436.
22. C.Trautmann, C.Dufour, E.Paumier, R.Spohr, M.Toulemonde. Track etching in amorphous metallic $Fe_{81}B_{13,5}Si_{3,5}C_2$ // *Nucl. Instr. and Meth. in Phys. Res. B.* 1996, v.107, p.397-402.
23. A.Audouard, E.Balanzat, J.C.Jousset, D.Lesueur, L.Tomé. Atomic displacements and atomic motion induced by electron excitation in heavy-

ion-irradiated amorphous metallic alloys // *J. Phys.: Condensed Matter.* 1995, v.5, №5, p.995-1018.
24. V.K.Semina, A.Yu.Didyk, V.A.Altynov. The changes in amorphous alloy under high energy heavy ions irradiation // *Structural principles of material modifications by unconventional technologies.* Proceedings of the 6th International Seminar (Obninsk, 12-15 June 2001). Obninsk, 2001, p.24-25 (in Russian).
25. V.K.Semina, A.Yu.Didyk, V.A.Altynov, A.L.Suvorov, A.S.Fedotov, Yu.N.Cheblukov, A.Khalil. Structural changes in amorphous alloys under irradiation with high energy heavy ions // *Radiation Physics of Solids.* Proceedings of the 11th International Conference (Sevastopol, 25-30 June, 2001). 2001, p.10-15 (in Russian).
26. M.Toulemonde. Nanometric phase transformation of oxide materials under GeV energy heavy ion irradiation // *Nucl. Instr. and Meth. in Phys.Res. B.* 1999, v.156, №1-4, p.1-11.
27. Ja.E.Gegusin, M.I.Kaganov, I.M.Lifshic. Electron free length effect on track formation around charged particle trajectory in metal // *Fizika Tverdogo Tela* (Rus.). 1973, v.15, №.8, p.2425-2428.
28. I.M.Lifshic, M.I.Kaganov, L.V.Tanatarov. On the theory of radiation changes in metals // *Atomic Energy* (Rus.). 1959, v.6, №4, p.391-402.
29. L.P.Biró, J.Gyulai, K.Havancsák, A.Yu.Didyk, L.Frey, H.Ryssel. In-depth damage distribution by scanning probe methods in targets irradiated with 200 MeV ions // *Nucl. Instr. and Meth. in Phys. Res. B.* 1997, v.127/128, p.32-37.
30. L.P.Biró, J.Gyulai, K.Havancsák, A.Yu.Didyk, S.Bogen, L.Frey. Use of atomic force microscopy and of a parallel irradiation geometry for in-depth characterization of damage produced by swift Kr ions in silicon // *Phys. Rev. B.* 1996, v.54, №17, p.11853-11856.
31. L.P.Biró, J.Gyulai, K.Havancsák, A.Yu.Didyk, S.Bogen, L.Frey, H.Ryssel. New method based on atomic force microscopy for in-depth characterization of damage in Si irradiated with 209 MeV Kr // *Nucl. Instr. and Meth. in Phys. Res. B.* 1997, v.122, №3, p.559-562.
32. L.P.Biró, G.I.Márk, J.Gyulai, K.Havancsák, S.Lipp, Ch.Lehrer, L.Frey, H.Ryssel. AFM and STM investigation of carbon nanotubes produced by high energy ion irradiation of graphite // *Nucl. Instr. and Meth. in Phys. Res. B.* 1999, v.147, №1-4, p.142-147.
33. L.P. Biró, B.Szabó, G.I.Márk, J.Gyulai, K.Havancsák, J.Kürti, A.Dunlop, L.Frey, H.Ryssel. Carbon nanotubes produced by high energy (E>100 MeV), heavy ion irradiation of graphite // *Nucl. Instr. and Meth. in Phys. Res. B.* 1999, v.148, p.1102-1105.
34. P.Nagy, B.Szabo, Zs.Szabo, K.Havancsák, L.P.Biró, J.Gyulai. Model of hillocks creation // *Ultramicroscopy.* 2001, v.86, p.31-35.

35.J.Liu, M.D.Hou, C.L.Liu, Z.G.Wang, Y.F.Jin, P.J.Zhai, S.L.Feng, Y.Zhang. Track of high energy heavy ions in HOPG studied with scanning tunneling microscopy // *Nucl. Instr. and Meth. in Phys. Res. B.*, 1998, v.146, №1-4, p.356-361.
36.A.Yu.Didyk, S.V.Latyshev, V.K.Semina, A.E.Stepanov, A.L.Suvorov, A.S.Fedotov, Yu.N.Cheblukov. Study on effect of 305 MeV krypton ions on high oriented pyrolytic graphite // *Letters to J. Techn. Phys.* (Rus.). 2000, v.26, №17, p.1-5.
37.Yu.N.Cheblukov, A.Yu.Didyk, A.S.Fedotov, S.V.Latyshev, V.K.Semina, A.E.Stepanov, A.L.Suvorov, N.A.Vasiliev. Surface structure changes of high oriented pyrolytic graphite under influence of swift heavy ions // *Advanced Materials*. 2001, №5, p.42-45.
38.S.Bouffard, J.Cousty, Y.Pennec, F.Thibaudan // *Rad. Eff. and Def. in Solids.* 1993, v.126, p.225.
39.H.Kemmer, S.Grafstrom, M.Neitzert, M.Wortge, R.Neumann, C.Trautmann, J.Vetter, N.Angert. Scanning tunneling microscopy of surface modifications induced by UNILAC heavy-ion irradiation // *Ultramicroscopy*. 1992, v.42-44, p.1345-1349.
40.*The properties of carbon-based structural materials*. Reference book, Ed. V.P.Mjasoedov. Moscow: Metallurgy, 1975 (in Russian).
41.Yu.N.Yavlinskii. Elastic interaction of MeV/amu heavy multicharged ions with solids // *Nucl. Instr. and Meth. in Phys. Res. B.* 1996, v.107, №1-4, p.83-86.
42.*Physical Parameters:* Reference Book, Eds. I.S.Grigoriev, E.Z.Meilikhov. Moscow: Energoatomizdat, 1991, 1232 pp. (in Russian).
43.D.V.Kulikov, A.L.Suvorov, R.A.Suric, Yu.V.Trushin, V.S.Kharlamov. Physical model of the periodic structure formation on the pyrolytic graphite surface under high-energy ion irradiation // *Letters to J. Tech. Phys.* (Rus.). 1993, v.23, №14, p.89-93.
44.Yu.N.Yavlinskii // *Rad. Eff. and Def. in Solids*, 2000, v.153, p.75.
45.P.I.Gaiduk, F.F.Komarov, V.S.Tishkov, W.Wesch, E.Wendler. Wurtzite InP formation during swift Xe-ion irradiation // *Phys. Rev. B.* 2000, v.61, №23, p.15785-15788.
46.P.I.Gaiduk, F.F.Komarov, W.Wesch. Damage evolution in crystalline InP during irradiation with swift Xe ions // *Nucl. Instr. and Meth. in Phys. Res. B.* 2000, v.164-165, p.377-383.
47.S.Furuno, H.Otsu, K.Hojou, K.Izui. Tracks of high energy heavy ions in solids // *Nucl. Instr. and Meth. in Phys. Res. B.* 1996, v.107, №1-4, p.223-226.
48.H.Huber, W.Assmann, S.A.Karamian, H.D.Mieskes, H.Nolte, E.Gazes, M.Kokkoris, S.Kossionides, R.Vlaston, R.Grötzshel, A.Mücklick, W.Prusseit. Heavy-ion induced damage of crystalline Ge and W in the 0.5-

8 A MeV range // *Nucl. Instr. and Meth. in Phys. Res. B.* 1998, v.146, №1-4, p.309-316.
49. S.A.Karamian, Yu.Ts.Oganessian, V.N.Bugrov. The effect of high-energy ions heavier than argon on a germanium single crystal and a new mechanism for autorecrystallisation // *Nucl. Instr. and Meth. in Phys. Res. B.* 1989, v.43, №2, p.153-158.
50. M.Chanel, J.Hansen, J.-M.Laurent, N.Madsen, E.Mahner. Experimental investigation of impact-induced molecular desorption by 4.2 MeV/u Pb ions // *Particles Accelerator Conference*, 18-22 June, 2001. CERN/PS 2001-040 (AE), 2001.
51. F.F.Komarov, A.P.Novikov, A.F.Burenkov. *Ion implantation.* Minsk, University, 1994, p.249 (in Russian).
52. A.Berthelot, S.Hemon, F.Geurbilleau, C.Dufour, E.Dooryhee, E.Paumier. Nanometric size effect on irradiation of tin oxide powder // *Nucl. Instr. and Meth. in Phys. Res. B.* 1998, v.146, №1-4, p.437-442.
53. A.Yu.Didyk, A.P.Kobzev, O.L.Orelovitch, V.K.Semina. Track effects in silicon irradiated by swift high energy heavy ions // *JINR Communication* E14-2000-107. Dubna, JINR, 2000.

Received on October 25, 2002.

Дидык А. Ю. и др.
E14-2002-243

Эволюция структуры поверхности твердых тел
при облучении тяжелыми ионами высоких энергий

Представлены результаты изучения изменений структуры поверхности твердых тел, таких как металлы, металлические сплавы, аморфные металлические сплавы и высокоориентированный пиролитический графит (ВОПГ), под действием облучения тяжелыми ионами ^{86}Kr (энергия ионов 245 МэВ, флюенсы облучения 10^{13}, 10^{14}, 10^{15} см$^{-2}$) и ^{209}Bi (энергия ионов 705 МэВ, флюенсы облучения 10^{12}, 10^{13} см$^{-2}$). Измерены коэффициенты распыления металлов (Ni, W, Au), нержавеющей стали Х18Н10, аморфного сплава $Ni_{58}Nb_{42}$ и ВОПГ. Показано, что коэффициенты распыления отожженных образцов поликристаллов (Ni, Au), как и монокристаллов (W, ВОПГ), при низкой концентрации дефектов относительно невелики. На этой стадии происходит преимущественное распыление границ зерен (Ni, ВОПГ). По мере накопления дефектов радиационного происхождения при флюенсах облучения порядка 10^{15} см$^{-2}$ коэффициенты распыления начинают значительно увеличиваться. Аналогичные результаты получены на аморфных сплавах, не имеющих дальнего порядка решетки (только ближний порядок), и на холоднодеформированных образцах золота. С ростом величины ионизационных (неупругих) потерь энергии начинают появляться кратеры на поверхности ВОПГ в местах прохождения ионов ^{209}Bi, но их концентрация составляет 2–3 % от флюенса ионов. Обсуждена феноменологическая модель указанного поведения.

Работа выполнена в Лаборатории ядерных реакций им. Г. Н. Флерова ОИЯИ.

Сообщение Объединенного института ядерных исследований. Дубна, 2002

Didyk A. Yu. et al.
E14-2002-243

Evolution of the Surface Structures of Solids under Irradiation
with High Energy Heavy Ions

The results on the study of surface structure of solids, like metals, metal alloys, amorphous metal alloys and highly oriented pyrolytic graphite (HOPG) under irradiation with heavy ^{86}Kr ions (ion energy is 245 MeV, irradiation fluences are 10^{13}, 10^{14}, 10^{15} cm^{-2}) and ^{209}Bi (ion energy is 705 MeV, irradiation fluences are 10^{12}, 10^{13} cm^{-2}) are presented. The sputtering coefficients for metals (Ni, W, Au), stainless steel Cr18Ni10, amorphous alloy $Ni_{58}Nb_{42}$ and HOPG are measured. It is shown that the sputtering coefficients of annealed polycrystals (Ni, Au) and single crystals (W, HOPG) are not large at low defect concentration in materials. At this stage, the sputtering of grain boundaries predominantly takes place. The sputtering yields become to increase significantly with the growth of damage concentration at ion fluences of the order of 10^{15} cm^{-2}. Analogous results were obtained for amorphous alloys, which do not have the long-range order (only short-range order), and for cold-deformed Au samples. When ionized energy loss increases, individual craters begin to appear on the irradiated surface of HOPG at the place of the passage of ^{209}Bi ions, but their concentration is about 2–3 % from ion fluence. The applicability of thermal spike model for the explanation of such behavior is discussed.

The investigation has been performed at the Flerov Laboratory of Nuclear Reactions, JINR.

Communication of the Joint Institute for Nuclear Research. Dubna, 2002

Редактор *С. Ю. Романов*
Макет *Е. В. Сабаевой*

Подписано в печать 27.12.2002.
Формат 60 × 90/16. Бумага офсетная. Печать офсетная.
Усл. печ. л. 1,63. Уч.-изд. л. 2,21. Тираж 290 экз. Заказ № 53686.

Издательский отдел Объединенного института ядерных исследований
141980, г. Дубна, Московская обл., ул. Жолио-Кюри, 6.
E-mail: publish@pds.jinr.ru
www.jinr.ru/publish/